New mathematical model for the Morton Effect based on the THD analysis

B. S. Grigor'ev[1], A. E. Fedorov[2] and J. Schmied[3]

[1] St. Petersburg State Polytechnical University, St. Petersburg, Russia
bsgrigoriev@gmail.com
[2] St. Petersburg State Polytechnical University, St. Petersburg, Russia
aleksandr.fml@gmail.com
[3] DELTA JS AG, Zurich, Switzerland
jschmied@delta-js.ch

Abstract. A new model for analyzing the Morton effect is presented. Previous studies of the Morton effect were either simplified or rigorously detailed requiring huge computational effort. The present work describes the new model which tries to combine accuracy of the model and computational efficiency. Perturbation method was used for the governing equations of the lubrication theory. The averaging method was applied to the equations of motion, facilitating large time steps for the numerical integration process, thus, greatly reducing the computational effort. The estimation of the spectral radius of transition operator was proposed as a convenient indicator for the rotordynamic system's stability threshold. As a concrete example a double overhung turboexpander supported on 5-pad tilting-pad bearings was considered, which has been previously studied experimentally and analytically by Schmied and others in 2008.

Keywords: Morton effect, synchronous thermal instability, spiral vibrations, differential heating, shaft's thermal bend.

1   Introduction

In the case of a residual unbalance in the rotor the journal will execute a small synchronous orbit. Then one part of the shaft surface will always be closer to the bearing wall than other parts. This causes a higher friction in this domain, because the shear stress is proportional to the velocity gradient, and leads to a non-uniform temperature distribution of the shaft in circumferential direction inside the bearing and ultimately to a thermal bend. This thermal bend can in combination with an overhung mass significantly increase the rotor unbalance and thus the synchronous rotor vibration. Under certain conditions this effect can lead to synchronous rotor instability. Such instability caused by asymmetrical bearing journal heating is known as the Morton effect and sometimes also referred to as the hot spot phenomenon.

In the meantime a significant number of papers devoted to the theoretical investigation of the Morton effect are published. A detailed overview of publications is presented in [1]. The publications can be divided into three groups. First are the analyti-

cal investigations (for ex. [2]). They are important, because they revealed the existence and some properties of the effect. On the other hand they are applicable to limited types of bearings. The second group are simplified models (for ex. [3, 4]), which are based on the estimations of some coefficients or on the solution of very simplified governing equations of the lubrication theory. Such models are easy to implement, but it is difficult to fully trust in their results due to the simplifying assumptions. Finally, the third group are models, which use a rigorous approach such as a CFD technique or a method described in [5]. The main problem of such approaches is a huge computational cost.

The present paper describes a new model for analyzing the Morton effect, which is quite rigorous and at the same time is computationally efficient. In the first stage of the modeling the static equilibrium position in the bearing is determined taking into account variable viscosity and cavitation. Based on solving a perturbed Reynolds equation the bearing dynamic coefficients are determined. In the second stage of the modeling the shaft's and pad's equations of motion considering the shaft's asymmetrical heating and thermal bending inside the bearing are solved. For the determination of the shaft's thermal bend the oil temperature is determined by solving the energy equation. The temperature distribution allows calculating the heat flow from oil to the shaft for one revolution of the rotor's synchronous response. This heat flow allows calculating the shaft asymmetrical heating and the subsequent shaft thermal bending. Using the averaging method for the equation of motion allows large time steps in the numerical integration process and, thus greatly reduces the computational effort. Numerical results for simulating the Morton effect are provided and compared with test data [6].

2 Theory

2.1 Governing Equations

The proposed model can be applied to bearings with different design. The focus of the current research is tilting pad bearings, since they are widely used for high speed applications, because they are generally more stable.

For the definition of the fluid film pressure distribution in each pad of the bearing the variable viscosity form of the Reynolds equation is used:

$$\frac{\partial}{\partial x}\left(F_2 \frac{\partial p}{\partial x}\right) + \frac{\partial}{\partial z}\left(F_2 \frac{\partial p}{\partial z}\right) = U\frac{\partial f_C}{\partial x} + \frac{\partial h}{\partial t}, \tag{1}$$

$$F_2 = \int_0^h \frac{y}{\mu}\left(y - \frac{F_1}{F_0}\right)dy, \quad F_0 = \int_0^h \frac{dy}{\mu}, \quad F_1 = \int_0^h \frac{ydy}{\mu}, \quad f_C = h - \frac{F_1}{F_0} \tag{2}$$

with h – film thickness, p – oil pressure, t – time, μ – oil viscosity, x, y, z – axes of the coordinate system.

The pressure at the leading edge of the each pad is the supply pressure. At the remaining boundaries of the film the pressure is atmospheric. In the case of cavitation the Swift-Stieber conditions are used.

For the determination of the oil temperature distribution for each pad the energy equation is solved. In the current research the energy equation is considered at the midplane of the bearing, assuming that the axial variation of the oil film temperature is negligible. Thus the following form of the energy equation is used

$$\rho c_p \left(\frac{\partial T}{\partial t} + u\frac{\partial T}{\partial x} + v\frac{\partial T}{\partial y} \right) = \mu \left(\frac{\partial u}{\partial y} \right)^2 + \frac{\partial}{\partial x}\left(\lambda \frac{\partial T}{\partial x} \right) + \frac{\partial}{\partial y}\left(\lambda \frac{\partial T}{\partial y} \right) \tag{3}$$

with ρ – oil density, c_p – heat capacity of oil, λ – heat conductivity of oil, u, v – circumferential and radial components of the oil velocity.

The energy equation is solved around the whole circumference of the bearing using the boundary layer theory to estimate the dissipation term between pads. For the heat exchange condition at the oil-pad interface the approach proposed in [7] is used. For the viscosity-temperature relationship the equation of Falz is used

$$\mu = \mu_0 \left(T/T_0 \right)^{-k} \tag{4}$$

with T_0 – reference temperature (usually it is an oil supply temperature), μ_0 – oil viscosity at temperature T_0, k – coefficient, which depends from the oil.

The Reynolds equation and the energy equation are coupled via the viscosity distribution. For the joint solution of these equations an iteration process is implemented, where the updated viscosity distribution, obtained from the solution of the energy equation (3) and viscosity-temperature relationship (4), is used for solving the Reynolds equation (1) at the next iteration step. The Reynolds and energy equations are solved by using the finite volume method.

The shaft temperature distribution is calculated by solving the 3D heat conduction equation in cylindrical rotating coordinate system (r, φ, z)

$$\frac{\partial T_s}{\partial t} = \frac{\lambda_s}{c_s \rho_s} \left(\frac{1}{r}\frac{\partial}{\partial r}\left(r\frac{\partial T_s}{\partial r} \right) + \frac{1}{r^2}\frac{\partial^2 T_s}{\partial \varphi^2} + \frac{\partial^2 T_s}{\partial z^2} \right) \tag{5}$$

with T_s – shaft temperature, ρ_s, c_s and λ_s – density, heat capacity and heat conductivity of the shaft's material.

For the numerical solution of equation (5) the splitting method is used. Here it is important to note, that equation (5) is solved not only within the limits of the bearing but also at some external domain of the bearing. The size of this domain is determined in the calculation process.

Any bend angle of the shaft at the bearing may be defined by $\beta_x(t,z)$ and $\beta_y(t,z)$ which are fixed to the shaft. For the definition of the bend angle purely caused by thermal influences the analysis developed by Dimarogonas [8] is adopted. This yields the following formula

$$\frac{d\beta}{dz} = -\frac{\alpha}{I} \int\limits_{0}^{2\pi} \int\limits_{0}^{R} T_s(t,\varphi,r,z) r^2 e^{i\varphi} d\varphi dr, \quad \beta = \beta_x + i\beta_y \tag{6}$$

with I – shaft's cross section second moment of area, R – shaft's radius and α – thermal expansion coefficient.

The flexible rotor is modeled with Timoshenko beam elements. The equation of motion for the rotor bearing system has the form

$$\mathbf{M\ddot{X}} + (\mathbf{D} + \mathbf{G})\mathbf{\dot{X}} + \mathbf{KX} = \mathbf{f}(t) \tag{7}$$

with $\mathbf{X}$ – system degree of freedom vector consisting of generalized deflections of the center of rotation at element nodes in a globally fixed coordinate system, $\mathbf{M}$ – mass matrix, $\mathbf{D}$ – damping matrix, $\mathbf{G}$ – gyroscopic matrix, $\mathbf{K}$ – stiffness matrix and $\mathbf{f}$ – external force.

If the rotor is thermally deformed the equation of motion for coordinates $\mathbf{X}$ relative to the static position of the undeformed rotor is ([2, 3, 5])

$$\mathbf{M\ddot{X}} + (\mathbf{D} + \mathbf{G})\mathbf{\dot{X}} + \mathbf{KX} = \mathbf{f}(t) + \mathbf{K_R X_T} , \tag{8}$$

where $\mathbf{K_R}$ is the stiffness matrix of the rotor alone (without bearings) and $\mathbf{X_T}$ is the vector describing the thermal deformation. Elements of the vector $\mathbf{X_T}$ are calculated using (6).

Equation (8) is complemented by the pad's equations of motions

$$\mathbf{I_{pad}\ddot{\psi}} + \mathbf{C_{\psi}X_b} + \mathbf{D_{\psi}\dot{X}_b} + \mathbf{E_{\psi}\psi} + \mathbf{H_{\psi}\dot{\psi}} = 0 \tag{9}$$

with $\mathbf{X_b}$ – shaft's deflection at the bearing's nodes; $\mathbf{\psi}$ – vector of the pad's tilt angles; $\mathbf{I_{pad}}$, $\mathbf{C_{\psi}}$, $\mathbf{D_{\psi}}$, $\mathbf{E_{\psi}}$, $\mathbf{H_{\psi}}$ – matrices of the inertia moments and dynamic coefficients of the pads.

2.2 Perturbation method

As it is known [1], the maximum temperature difference due to asymmetrical heating of synchronously precessing shaft is small compared to the temperature level in the lubricant film. At the same time errors arise, due to the approximate description of the physical process in the system and the used computational methods. As a result, the total error can have the same order of magnitude as the studied effect. In order not to "lose" the effect, the perturbation method is used.

The film thickness for an arbitrary position of the shaft can be presented as sum of the thickness in equilibrium position and an additional term

$$h = h_0 + \delta h . \tag{10}$$

Due to smallness of the initial unbalance and, accordingly, smallness of the resulting vibration, δh is a small value compared with h_0. In accordance with the perturbation

method the oil pressure can be found as sum of the pressure in equilibrium position and a "perturbed" term

$$p = p_0 + \delta p .$$ (11)

The oil velocity components u and v, the oil temperature T and the shaft temperature T_s can be written in a similar way. Neglecting terms of second order and higher, the governing equations splits on the equations of zeroth and first order. Zeroth order equations for p_0, T_0 etc. correspond to the static equilibrium position. Perturbed (first order) equations for δp, δT etc. correspond to the shaft vibration around the static equilibrium position due to initial mechanical unbalance.

2.3   Averaging method

Harmonic excitation is considered as an initial unbalance. In this case $\mathbf{f}(t)$ and $\mathbf{X_T}$ in (8) can be written in the form

$$\begin{aligned}
\mathbf{f}(t) &= \mathbf{f_c} \cos(\omega t) + \mathbf{f_s} \sin(\omega t) \\
\mathbf{X_T} &= \mathbf{X_T^c}(t) \cos(\omega t) + \mathbf{X_T^s}(t) \sin(\omega t)
\end{aligned}$$ (12)

with ω - angular shaft's speed. Due to the gradual heating of the shaft, $\mathbf{X_T^c}$ and $\mathbf{X_T^s}$ are time dependent (in contrast with $\mathbf{f_c}$ and $\mathbf{f_s}$, which are constant in time). That's why taking into account (12), the solution of (8) and (9) is searched in the form (synchronous precession)

$$\begin{cases} \mathbf{X} = \mathbf{X_c}(t) \cos(\omega t) + \mathbf{X_s}(t) \sin(\omega t) \\ \mathbf{\psi} = \mathbf{\psi_c}(t) \cos(\omega t) + \mathbf{\psi_s}(t) \sin(\omega t) \end{cases},$$ (13)

where $\mathbf{X_c}$, $\mathbf{X_s}$, $\mathbf{\psi_c}$ and $\mathbf{\psi_s}$ are not constant but slowly varying in time due to the shaft heating. Physically it is clear, that this variation is much slower than one period of the shaft revolution.

Applying the idea of the method of variation of parameters (variation of constants) it is possible to receive the first order equations for $\mathbf{X_c}$, $\mathbf{X_s}$, $\mathbf{\psi_c}$ and $\mathbf{\psi_s}$. As written above $\mathbf{X_c}$, $\mathbf{X_s}$, $\mathbf{\psi_c}$ and $\mathbf{\psi_s}$ change in time much slower than $cos(\omega t)$ and $sin(\omega t)$ and can be considered as constants over one period of revolution. Proceeding from this and averaging the right hand sides of the first order exact equations for $\mathbf{X_c}$, $\mathbf{X_s}$, $\mathbf{\psi_c}$ and $\mathbf{\psi_s}$ over one period, the following system of the averaging equations is received

$$\begin{aligned}
-2\mathbf{M}\omega\dot{\mathbf{X}}_\mathbf{c} - \omega(\mathbf{D}+\mathbf{G})\mathbf{X_c} + \left(\mathbf{K} - \mathbf{M}\omega^2\right)\mathbf{X_s} &= \mathbf{f_s} + \mathbf{K_R}\mathbf{X_T^s} \\
2\mathbf{M}\omega\dot{\mathbf{X}}_\mathbf{s} + \omega(\mathbf{D}+\mathbf{G})\mathbf{X_s} + \left(\mathbf{K} - \mathbf{M}\omega^2\right)\mathbf{X_c} &= \mathbf{f_c} + \mathbf{K_R}\mathbf{X_T^c}
\end{aligned}.$$ (14)

The equations for $\mathbf{\psi_c}$ and $\mathbf{\psi_s}$ are derived similarly.

The resulting equations (14) are solved by the trapezoidal method and the integration step corresponds to a step used for the determination of shaft's thermal bend. This step is equal to the time of a few shaft's revolutions. Thus using the averaging

method allows using a much bigger time step and to implement a much less time consuming scheme in comparison to a direct integration of (8) and (9).

Similar to (13) the perturbed oil temperature can be writing in the form

$$\delta T = T_c(t)\cos(\omega t) + T_s(t)\sin(\omega t) . \tag{15}$$

Here T_c, T_s changes in time much slower than $cos(\omega t)$ and $sin(\omega t)$ as in the case of the vibration parameters. Continuing the idea of the averaging method, T_c, T_s are considered as constants in time during the time step (few shaft's revolutions), which is used for solving (14). Finally, representation (15) allows simplifying the numerical procedure for the perturbed energy equation, because instead of one transient equation it is possible to solve two coupled stationary equations for T_c and T_s. This system of differential equations is solved by using the finite volume method.

2.4   General Scheme of calculations. Spectral radius of transition operator

Figure 1 provides the general flow chart for the calculating process according to the described scheme for the Morton effect analysis.
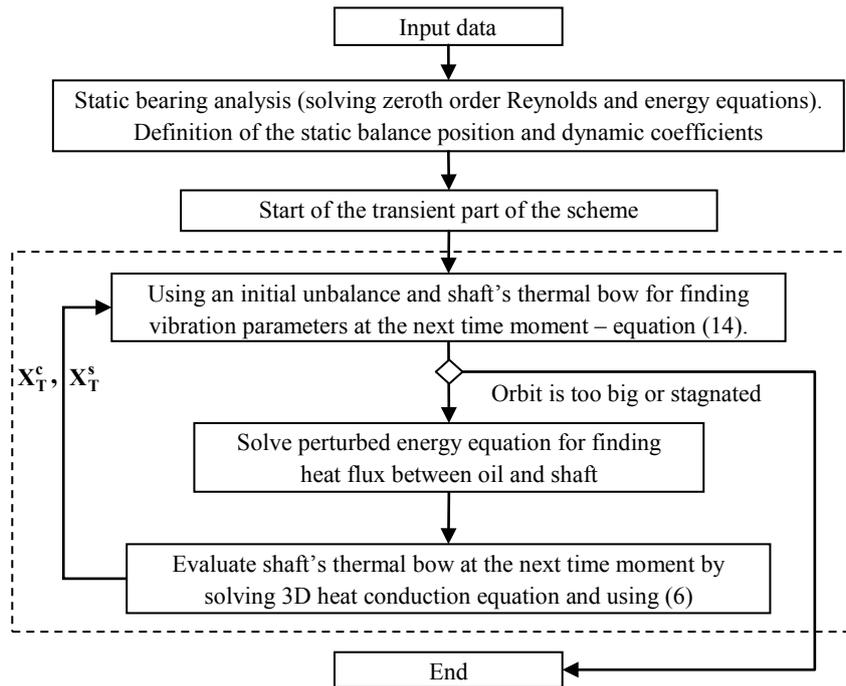
Fig. 1. Flow chart: transient analysis of the Morton effect

Here it is important to note that the transient part of the scheme (marked by dashed rectangle at fig. 1) is the solution of the Cauchy problem for the equation (14), where

it is necessary for the determination of the right-hand part at each time step to solve the perturbed energy equation in the lubricant film, which is coupled through the heat flux with the heat conduction equation for the shaft.

Due to the numerical methods, which were used during the design of the described model the resulting discrete problem that approximates the original continuous problem (marked by dashed rectangle at fig. 1) has the form

$$\mathbf{r_{n+1}} = \mathbf{R}\mathbf{r_n} + \mathbf{d} \ , \tag{16}$$

where $\mathbf{R}$ is an transition operator which corresponds to the implementation of the one time step of the process, $\mathbf{r}$ is a vector which contains all unknown shaft's vibration parameters, n is a number of the time step. For the stability of the discrete problem it is necessary and sufficient that $\rho(\mathbf{R}) < 1$, where $\rho(\mathbf{R})$ is a spectral radius of operator $\mathbf{R}$. For the approximation of the original continuous problem unconditionally stable methods were used. Therefore the only source for instability in the computational process (16) is the instability of original problem. Since for sufficiently small parameters of discretization (sizes of grid cells) solutions of discrete and continuous problems are close it is possible to suppose that condition $\rho(\mathbf{R}) < 1$ will approximately define the stable region as discrete and continuous problems. Condition $\rho(\mathbf{R}) = 1$ will give the stability threshold. Thus the estimation of the spectral radius can be a convenient indicator for the stability in the analysis of the Morton effect.

Since $\mathbf{R}$ is a finite dimensional operator, its spectral radius is the maximum modulus of the eigenvalues of the corresponding matrix, which is explicitly unknown. However implicitly this matrix is present in the calculation process and its spectral radius can be calculated by the power method.

3 Results

3.1 A Case Study

The described mathematical model was applied to the analysis of the Morton effect for the rotor with two overhung impellers of the turboexpander TC 400/90 made by Cryostar SAS [6]. This is a typical system with high hot spot sensitivity. The described machine is supported by two 5-pad tilting pad bearings with load-on-pad. The rotor of the turboexpander is shown in fig. 2. The total shaft length is 760 mm, the total rotor mass is 120.63 kg.
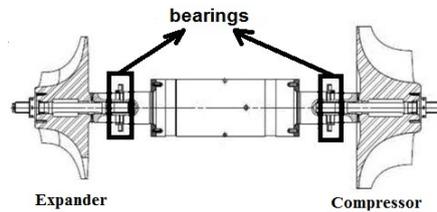
Fig. 2. Rotor system of the turboexpander TC 400/90 [6]

During the internal testing of the turboexpanders the measured shaft vibration started to rise suddenly just above the nominal speed (~18000 rpm). The vibration had a dominant (1×N) component. The vibration polar plot had the spiral vibration appearance typical for the Morton effect.

In the process of calculation an initial mechanical unbalance with a magnitude of 4 times the API residual unbalance (165 gmm) [9] is used. The unbalance magnitude is based on the complete rotor weight, not just on the overhung portions.

3.2 Calculation results

In fig. 3 the polar plots (amplitude and phase) of the calculated vibration for different rotational speeds are presented. The result of the vibration in the compressor bearing is shown.
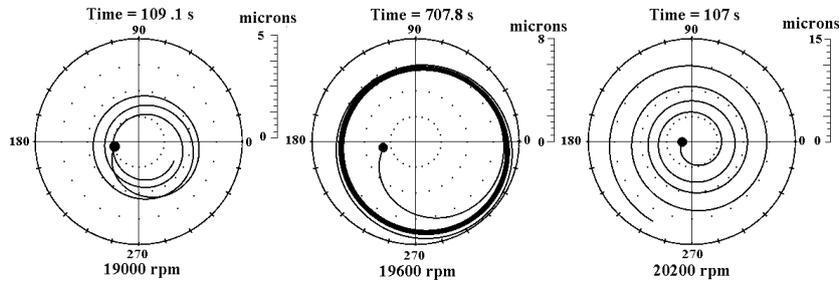
Fig. 3. Spiral vibration in polar plot, which was calculated according to the described scheme

As can be seen from the presented figures, the change of amplitude and phase with time in the polar plot has the spiral form typical for the Morton effect. In each graph the small black circle corresponds to the start of calculation process, i.e. to the vibration amplitude and phase only due to initial mechanical unbalance. It can be seen, that the speed 19000 rpm lays in the stable zone (spiral with decreasing amplitude), 19600 rpm corresponds practically to stability threshold and 20200 rpm is in unstable zone (spiral with increasing amplitude).

As it is known the cause of the shaft's thermal bend in the case of the Morton effect is asymmetrical heating inside the bearings. In fig. 4 the perturbed shaft surface temperature distribution in the surroundings of the bearing at the compressor side at the instant t = 120 seconds since the beginning of the calculation for the case of 19600 rpm is presented. The bearing boundaries are marked by solid bold lines. Thin solid lines are isotherms with temperature values marked on them. Two spots – cold (dark) and hot (bright) are clearly visible on the surface of the shaft. Such spots are typical for the Morton effect.

Above in the paper the spectral radius of transition operator was proposed as an indicator to assess the stability of the rotordynamic system in case of the Morton effect. In the left graph of fig. 5 the calculated spectral radius according to the described scheme is presented as a function of speed.
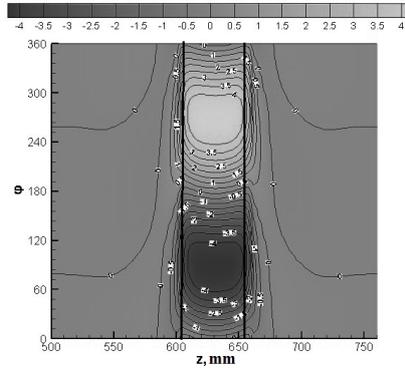
Fig. 4. Development of the perturbed shaft's surface temperature (bearing and its surroundings)
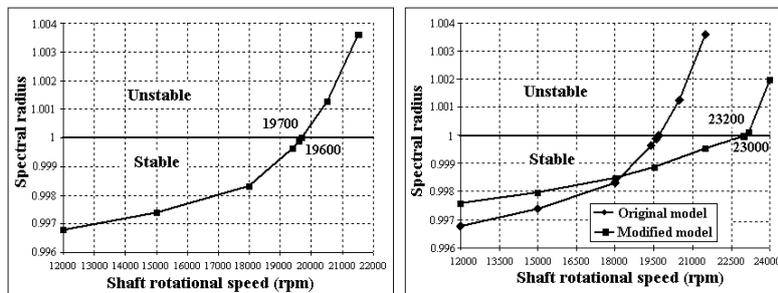
Fig. 5. Spectral radius as function of the rotational speed. Left graph - original model, right graph - original model vs. modified model

It is possible to see from fig. 5 that the stability threshold is at ~19690 rpm. This result is consistent with the conclusions based on the analysis of the spiral vibration in the polar plots in fig. 3. If we take the rotational speed of 18000 rpm as stability threshold of the real machine (starting from this speed there was a strong increase of the vibration level in the test), the results received on the base of the developed model differ from the test by less than 10%.

To prevent the Morton effect the manufactures of the turboexpander decided to make some modifications. At first they reduced the bearing width. The original tilting pad radial bearings had a width of 0.6D. It was decided to narrow the bearing width from 55 to 40 mm. In addition to the bearing width the oil viscosity was reduced from nominal 46 cSt to 32 cSt.

With the modified bearings and the oil viscosity reduction the test results did not show spiral vibrations anymore. The shaft thermal bow due to the hot spot phenomenon and spiral vibration were not observed up to speed of 22000 rpm. The results of the calculations with the described scheme are presented in the right graph of fig. 5. According to them, the calculated stability threshold for the modified system is equal to 23000 rpm. This result is fully agrees with the test.

4   Conclusions

A new model for analyzing the Morton effect has been presented. The spectral radius of the transition operator as a convenient indicator for stability in the analysis of the Morton effect is proposed. The results are well consist with experimental data. Using the averaging method reduced computational cost. With the chosen grid parameters the calculation of 1 second of the real process requires about 8.5 seconds processor time. That's why for the calculation of ~100 seconds of the real process (as at the two side graphics in the fig.3) requires about 14 minutes. At the same time using the spectral radius for the estimation of the system stability reduces calculation time. One point in fig. 5 needs about 4 - 6 minutes.

REFERENCES

1. de Jongh, F.: The Synchronous Rotor Instability Phenomenon – Morton Effect. In: Proceedings of the 37th Turbomachinery Symposium, pp. 159-167. Texas (2008).
2. Keogh, P.S., Morton, P.G.: Journal Bearing Differential Heating Evaluation with Influence on Rotor Dynamic Behaviour. In: Proc. of Royal Society. Series A. Vol. 441, pp. 527-548 (1993).
3. Schmied, J.: Spiral Vibrations of Rotors. In: Proc. 11th Biennial ASME Design Engineering Div. Conf., Vib. Noise, DE-Vol. 2 "Rotating Machinery Dynamics", pp. 449-456. Boston MA (1987).
4. Kirk, R.G., Zenglin, G., Balbahadur, A.C.: Synchronous Thermal Instability Prediction For Overhung Rotors, In: Proceedings of the 32nd turbomachinery symposium, pp. 121-135. Texas (2003).
5. Palazzolo, A., Lee, J.G.: Morton Effect Cyclic Vibration Amplitude Determination for Tilt Pad Bearing Supported Machinery. ASME Journal of Tribology, 135(1), 12 pages (2013).
6. Schmied, J., Pozivil, J., Walch, J.: Hot Spots in Turboexpander Bearings: Case History, Stability Analysis, Measurements and Operational Experience. In: Proceedings of ASME IGTI Turbo Expo 2008: Power for Land, Sea and Air, Vol. 5 Parts A and B, pp. 1267 - 1277. Berlin (2008).
7. Suganami, T., Szeri A.Z.: A Thermohydrodynamic Analysis of Journal Bearings. ASME Journal of Lubrication Technology, 101a, 21-27 (1979).
8. Dimarogonas, A.D.: Packing Rub Effect in Rotating Machinery, PhD thesis, Rennselaer Polytechnic Institute, Troy, New York (1970).
9. API 617: Axial and Centrifugal Compressors and Expander-compressors for Petroleum, Chemical and Gas Industry Services, 7th edition, API American Petroleum Institute (2002).